

ISO OBSERVATIONS OF THE INFRARED CONTINUUM OF THE HERBIG Ae/Be STARS

D. Elia, F. Strafella, L. Campeggio

Dipartimento di Fisica - Università di Lecce
Via per Arnesano C.P. 193 I-73100 Lecce - Italy
E-mail:¹eliad@le.infn.it

Abstract

We present a study of the whole sample of the Herbig Ae/Be stars observed with the spectrometers on board of the Infrared Space Observatory (ISO/ESA). These objects have been studied not only by means of their infrared continuum emission but also with respect to all the available photometric data, collected from the optical region to the radio wavelengths. The global spectral energy distributions (SEDs) have been compared with the results of radiative transfer calculations, that have been made in the framework of a circumstellar (CS) model. The results of the selection of the best models allow us to infer on the relationship between the geometry of the CS matter distribution and the evolutionary stage of these objects.

KEYWORDS: *stars: pre-main sequence – circumstellar matter – infrared: stars*

1. Observations, data reduction and results

The ISO data archive has been searched for Short Wavelength Spectrometer (SWS) and Long Wavelength Spectrometer (LWS) observations related to Herbig AeBe stars (HAeBe stars hereinafter). We found 36 objects (out of 108 stars recognized in Thé et al. (1994)), which are listed in Table 1.

Table 1: The observed sample of HAeBe stars

LkH α 198	Z CMa	He 3-1191	WW Vul
V376 Cas	HD 97048	HD 150193	BD +40°4124
Elias 3-1	HD 100546	CoD -42°11721	LkH α 224
AB Aur	HD 104237	HD 163296	PV Cep
MWC 480	IRAS 12496-7650	MWC 297	HD 200775
HD 34282	HD 141569	MWC 300	V645 Cyg
HD 36112	HD 142666	TY CrA	LkH α 234
CQ Tau	HD 144432	R CrA	LkH α 233
MWC 137	HR 5999	HD 179218	MWC 1080

The SWS spectra we discuss here were taken in the range 2.3–45 μm with low resolution ($\lambda/\Delta\lambda \sim 250$) and a typical field of view increasing with wavelength from $14'' \times 20''$ to $20'' \times 33''$ (De Graauw et al., 1996), while the LWS spectra were obtained in the range 43–196.7 μm , $\lambda/\Delta\lambda \sim 200$, (Clegg et al., 1996). In the LWS spectral range the instrumental beam size is $\sim 80''$ so that in some cases (12 objects) the observations were carried out also at an off-source position to account for the contamination due to the local background.

The raw SWS and LWS data were processed using version 10 of the off-line pipeline, which produced series of repeated spectral scans, each composed of 12 and 10 subspectra for SWS and LWS, respectively. These correspond to different spectral ranges, that are arranged to be partially overlapping. The data were further reduced and analysed in subsequent steps:

- removing bad points (glitches, residual detectors responsivity drifts);
- averaging of the many scans obtained on each subspectrum;
- removing of the low-frequency fringes, whose presence affects particularly the LWS spectra (Swinyard et al., 1998).
- smoothing of averaged spectra (SWS only).

Whenever possible, the off-source LWS spectra were subtracted from the corresponding on-source data. Notwithstanding accurate data reduction, the subspectra obtained appear in many cases not perfectly overlapping together, probably because of the variation of the beam size with the wavelength (De Graauw et al., 1996; Swinyard et al., 1998). In Fig. 1. we show examples of two reduced source spectra.

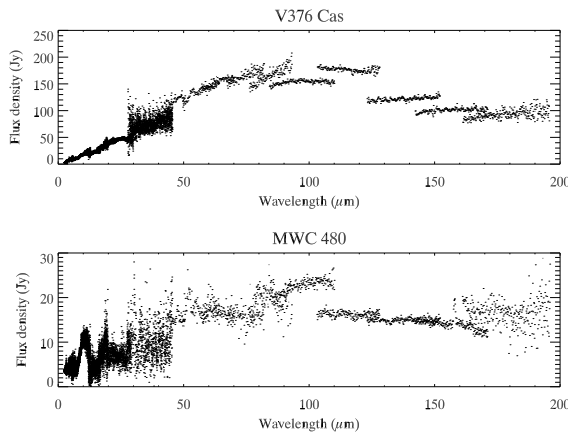


Figure 1: ISO spectra. Both sources show a good continuity between SWS and LWS fluxes despite the different beam-sizes involved. On the other hand they clearly present discontinuities in the LWS respective subspectra.

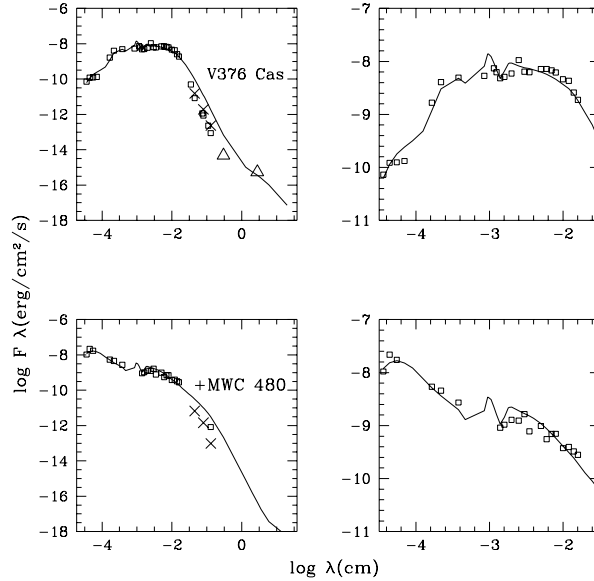


Figure 2: Spectral fits. Computed SEDs (solid line) are superimposed on the observed fluxes (circles, triangles are upper limits). Crosses represent submillimetric model fluxes corrected for diffraction effects due to the instrumental beamsize.

2. Model calculation and comparison with observations

The SEDs emerging from CS envelopes have been computed by means of a model based on a spherical geometry of the circumstellar environment. The model is characterized by a density distribution $n(r)$ around a central star and by the presence of an HII region whose radius is determined by the ionizing luminosity of the central star. A temperature profile $T(r)$ is also considered for the dust component while for the gas we assumed $T = 10^4$ K in the HII region. The gas emission processes considered in the radiation transfer are: free-free, free-bound and electron scattering, while for the dust component the emissivity is computed on the basis of the “astronomical silicate” defined by Draine & Lee (1984). Cases with a modified dust emissivity (at $\lambda > 20\mu\text{m}$) have also been computed to take into account the fact that in star forming regions the average dust grain size can be larger than in the diffuse IS medium and consequently the opacity can be described by a $k \propto \lambda^{-\beta}$ law; in our case, $\beta = 1.2, 0.8, 0.6$ (see Pezzuto et al. (1997) for a more complete model description). In addition we also consider:

- 1) the possible presence of cavities in the CS envelope as can be evacuated by the strong stellar wind associated with the PMS phases;

- 2) the possibility of two different density distributions describing the inner and outer parts of the envelope, respectively.

A large set of synthetic spectra has been computed; for each object we searched for the best fit with the observed fluxes. Such a comparison, made by means of a “chi square like” method, allows the selection of the best models for each object. In doing this we considered not only the spectral fit but also the consistency of the model fluxes with the spectral type estimated for the star, the distance, and the observed visual absorption. An example of the results obtained is presented in Table 2. and shown in Figure 1..

Table 2: Fit parameters and correspondent observables

Source	β	q	p	n_0 (cm^{-3})	Spectral type		A_V (mag)			Distance (pc)	
					Calc.	Obs.	CS	IS	Obs.	Calc.	Obs.
V376 Cas	1.2	0.5	0.8	$3 \cdot 10^8$	B5	B5	4	2.5	2.9-5.2	724 ± 32	600
					(1)				(3,4)		(3)
MWC 480	0.6	0.6	1.3	$3 \cdot 10^{10}$	A3	A3	1	0	0.25-0.4	101 ± 5	131
					(2)				(5,6)		(5)

NOTES: V376 Cas was fitted with a simple spherical model, MWC 480 with a model considering also two polar cavities.

REFERENCES TO THE TABLE: 1. Herbig & Bell (1988); 2. Jaschek et al. (1991); 3. Hillenbrand et al. (1992); 4. Pezzuto et al. (1997); 5. van den Ancker et al. (1998); 6. Miroshnichenko et al. (1999).

References

- Clegg, P.E., Ade, P.A.R., Armand, C., et al., 1996, A&A 315, L38
 De Graauw, T., Haser, L.N., Beintema, D.A., et al., 1996, A&A 315, L49
 Draine, B.T., Lee, H.M., 1984, ApJ 285, 89
 Herbig, G.H., & Bell, K.R., 1988, Lick Obs. Bull., 1111
 Hillenbrand, L.A., Strom, S.E, Vrba, F.J., Keene, J., 1992, ApJ 397, 613
 Jaschek, M., Jaschek, C., Andrillat, Y., 1991, A&A 250, 127
 Miroshnichenko, A., Ivezić, Z., Vinković, D., & Elitzur, M., 1999, ApJ, 520, L115
 Pezzuto, S., Strafella, F., Lorenzetti, D., 1997, ApJ 485, 290
 Swinyard, B.M., Burgdorf, M.J., Clegg, P.E., Davis, G.R., Griffin, M.J., Gry, C.,
 Leeks, S.J., Lim, T.L., Pezzuto, S., Tommasi, E., 1998. In: Proc. SPIE, A.M.
 Fowler (Ed.), Vol. 3354, p.888
 Thé, P.S., de Winter, D., Pérez, M.R., 1994, A&AS 104, 315
 van den Ancker, M.E., de Winter, D., Tjin A Djie, H.R.E., 1998, A&A 330, 145